The Beta-Ray Spectra of Europium and Tungsten

FRANKLIN B. SHULL*
Randall Laboratory of Physics, University of Michigan, Ann Arbor, Michigan
(Received June 18, 1948)

The primary function of this paper is to report the results of a spectrometric investigation of beta- and gamma-radiations from certain isotopes of europium and tungsten. A secondary function is to publish information concerning the design and operation of the magnetic double-focusing beta-ray spectrometer with which the investigation was carried out. The spectra for europium and tungsten serve also to illustrate the performance of the instrument.

THE magnetic double-focusing beta-ray spectrometer was first proposed by Siegbahn and Svartholm,[1] who subsequently published a number of papers[2] in which were presented the focusing theory and a discussion of the resolving power for this instrument. Somewhat later, Dennison and Shull,[3] working independently, developed the focusing theory by perturbation methods which were complete through the second order of approximation. Some results from this development are repeated below for convenience. A letter by Rosenblum[4] pointed out certain of the characteristics of the focused image as a function of small second-order variations in the shape of the magnetic field.

The essential features of the double-focusing spectrometer can be summarized as follows. The magnetic field is inhomogeneous, but it has both cylindrical symmetry about a vertical axis and mirror symmetry with respect to a horizontal plane (the median plane). In the development of the focusing theory by Dennison and Shull,[3] the field in the median plane was assumed to have the form

$$H=H_0[1-\tfrac{1}{2}(r-a/a)+\beta(r-a/a)^2], \qquad (1)$$

where H_0 = a constant, r = radius from the symmetry axis, a = radial coordinate of the radioactive source, and β = an arbitrary dimensionless constant which determines the second order contribution to the field. To first order, the magnetic field in the median plane falls off radially as $r^{-\frac{1}{2}}$. The presence of the arbitrary constant β allows, in second order, deviations from the $r^{-\frac{1}{2}}$ law.

Expressed in cylindrical coordinates, the trajectory of a beta-particle in the spectrometer is given by the equations

$$r=a+\delta r\cos\frac{\omega t}{\sqrt{2}}+\sqrt{2}a\varphi_r\sin\frac{\omega t}{\sqrt{2}}$$
$$+(\text{second order terms involving }\beta). \qquad (2)$$

$$z=\delta z\cos\frac{\omega t}{\sqrt{2}}+\sqrt{2}a\varphi_z\sin\frac{\omega t}{\sqrt{2}}$$
$$+(\text{second order terms involving }\beta). \qquad (3)$$

In Eqs. (2) and (3), the quantities ω, δr, δz, φ_r, and φ_z are defined as

$$\omega=-eH_0/mc\mp v/a,$$
$$r_0=a+\delta r,$$
$$z_0=\delta z,$$
$$(\dot{r})_0/v=\varphi_r,$$
$$(\dot{z})_0/v=\varphi_z,$$

where r_0, z_0, $(\dot{r})_0$, and $(\dot{z})_0$ are the coordinates and component velocities of the beta-particle at time $t=0$, when the particle is emitted from the source with total velocity v. With a radioactive source of restricted dimensions, δr and δz are both small compared to a. Thus electrons of the proper energy, emerging from a small source located approximately at $r=a$ and $z=0$, follow trajectories which execute, in general, simultaneous radial and vertical sinusoidal oscillations about the circle $r=a$ in the median plane. Since the two oscillations are in phase with one another, a rather sharp image of the source will be formed after one half-cycle of each, when the angular argument $\omega t/\sqrt{2}=\pi$. The image is displaced from the source through an angle $\theta=\omega t=\pi\sqrt{2}=254°\,33'$.

* Now at Washington University, St. Louis, Missouri.
[1] K. Siegbahn and N. Svartholm, Nature **157**, 872 (1946).
[2] K. Siegbahn and N. Svartholm, Arkiv. f. Mat., Astr. o. Fysik **33A**, No. 21 (1946); N. Svartholm, Arkiv. f. Mat., Astr., o. Fysik **33A**, No. 24 (1946).
[3] F. B. Shull and D. M. Dennison, Phys. Rev. **71**, 681 (1947); **72**, 256 (1947).
[4] E. S. Rosenblum, Phys. Rev. **72**, 731L (1947).

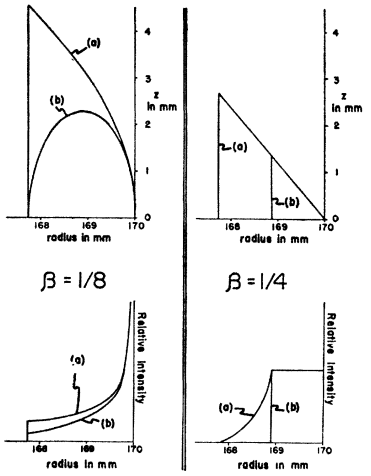

FIG. 1. Image of a point source.

Upper pictures: geometrical areas to which electrons from a monoenergetic point source are focused, with (a) square baffle aperture, and (b) circular aperture.
Lower pictures: intensity distributions across the images pictured above. See text for details.

A very advantageous characteristic of the double-focusing spectrometer has been pointed out by Siegbahn and Svartholm,[2] namely its high linear dispersion. Linear dispersion may be defined as the radial shift Δr in the position of the image of a monoenergetic source when the electron momentum is changed by a small quantity Δp. As shown by Siegbahn and Svartholm,

$$\Delta r \cong 4a(\Delta p/p)$$

for double-focusing, whereas

$$\Delta r = 2a(\Delta p/p)$$

for conventional 180° focusing. This fact leads one immediately to expect a higher resolving power for the double-focusing instrument.

As was shown in the earlier paper,[3] the second-order terms in Eqs. (2) and (3) are essentially "defocusing" terms, which can be minimized (but not completely eliminated) by a careful choice of the arbitrary parameter β. Rosenblum[4] demonstrated that the width of the focused image can be minimized by choosing $\beta=\frac{1}{4}$. However, as a result of an unfortunate error in the early stages of developing the focusing theory, the parameter was chosen to be $\beta=\frac{1}{8}$ for the spectrometer which was built and which is described in this paper. It is of interest, therefore, to investigate the expected performance of a double-focusing spectrometer for both choices for β, and to compare the results with the operational characteristics of the instrument which was constructed.

Let r^* and z^* be the coordinates of an electron at the image position, i.e., when $\omega t/\sqrt{2}=\pi$. Then, for $\beta=\frac{1}{8}$ and $\beta=\frac{1}{4}$, Eqs. (2) and (3) become

$$\begin{aligned} &\beta=\tfrac{1}{8} \\ &r^*=a-\delta r+\delta r^2/2a-5\delta z^2/6a-(4a/3)\varphi_z^2, \\ &z^*=-\delta z+\delta r\delta z/3a-(8a/3)\varphi_r\varphi_z, \end{aligned} \tag{4}$$

and

$$\begin{aligned} &\beta=\tfrac{1}{4} \\ &r^*=a-\delta r+\delta r^2/3a-2\delta z^2/3a-2a(\varphi_r^2+\varphi_z^2)/3, \\ &z^*=-\delta z+(2\delta r\delta z/3a)-(4a/3)\varphi_r\varphi_z. \end{aligned} \tag{5}$$

Using Eqs. (4) and (5), the questions of image formation, line shape, and resolving power can be investigated by graphical methods. In the analysis which follows, the computations assume spectrometer dimensions corresponding to the instrument built for this research. This means that

$$\begin{aligned} a&=170 \text{ mm}, \\ |\varphi_r|&\leqq 0.1 \text{ radian}, \\ |\varphi_z|&\leqq 0.1 \text{ radian}. \end{aligned}$$

The limitations on $|\varphi_r|$ and $|\varphi_z|$ are imposed by a square aperture in a baffle wall located halfway between the electron source and the focus position, i.e., at $\theta=\omega t=\pi/\sqrt{2}$. That this is so (in first approximation) may be seen by substituting $\omega t=\pi/\sqrt{2}$ into Eqs. (2) and (3). This gives

$$\begin{aligned} r&=a+\sqrt{2}a\varphi_r+\text{second order terms}, \\ z&=\sqrt{2}a\varphi_z+\text{second order terms}, \\ \theta&=\pi/\sqrt{2}. \end{aligned} \tag{6}$$

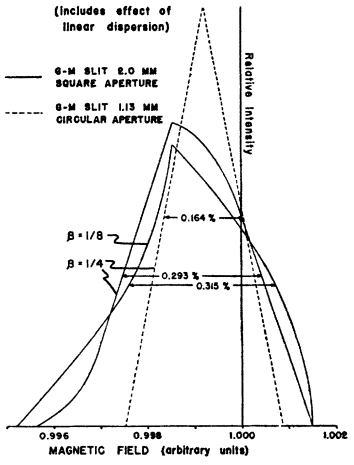

FIG. 2. Apparent line shape from a monoenergetic point source, with various choices for β and for the aperture shape.

If $|r|$ and $|z|$ in Eqs. (6) are limited by a baffle aperture, similar restrictions are imposed on $|\varphi_r|$ and $|\varphi_z|$ as a consequence.

In addition to the conditions outlined above, computations have been made also for the case of a different limitation on φ_r and φ_z, namely

$$(\varphi_r^2+\varphi_z^2)^{\frac{1}{2}}\leqq 0.1 \text{ radian.}$$

This is the case of a circular aperture in the baffle wall at $\omega t=\pi/\sqrt{2}$. The area of this circular aperture is $\pi/4$ times the area of the square aperture described previously.

The results of a graphical analysis of image formation are shown in Figs. 1, 2, and 3. Figure 1 illustrates the geometrical areas into which electrons from a monoenergetic point source (situated at $\delta r=\delta z=0$) are focused, under the condition of unchanging magnetic field ($H_0=$constant). These areas are located in the plane $\theta=\pi\sqrt{2}$. It should be emphasized that intensity is not uniform over these areas; the lower drawings of Fig. 1 illustrate this fact. They represent the counting rate observed from a Geiger counter with a high vertical entrance window of infinitesimal width, as the window is moved radially across the images in equal increments of distance. Of particular interest is the "block" distribution for the case $\beta=\frac{1}{4}$ and circular aperture.

Figure 2 illustrates the apparent line shape to be expected in actual operation of the spectrometer when the electrons originate from a monoenergetic point source (again at $\delta r=\delta z=0$). Here a Geiger counter with a high entrance window of finite width is assumed to be fixed at $r=a$, and the magnetic field H_0 is varied. The observed counting rate is plotted as a function of the magnetic field strength. Into Fig. 2 has gone all of the information contained in Fig. 1, plus the additional effect of linear dispersion. A Geiger tube slit width of two millimeters is used in the prototype spectrometer. Figure 2 indicates that the maximum resolving power to be expected from the prototype instrument under the most ideal conditions is 0.315 percent. With $\beta=\frac{1}{4}$, circular baffle aperture, and slit width of 1.13 millimeters, the maximum resolving power would be 0.164 percent.

If an infinitesimally narrow vertical *line* source is assumed in place of a point source, Fig. 2 would not be altered appreciably. This can be understood by examining Eqs. (6) again. In first approximation, neither δr nor δz appears in Eqs. (6). This means in effect that the limitations on φ_r and φ_z will be the same for all points in a vertical line source, even one of finite width. Thus, except for relatively small second-order contributions depending on δr and δz, the apparent line shapes illustrated in Fig. 2 hold equally well for a vertical line source.

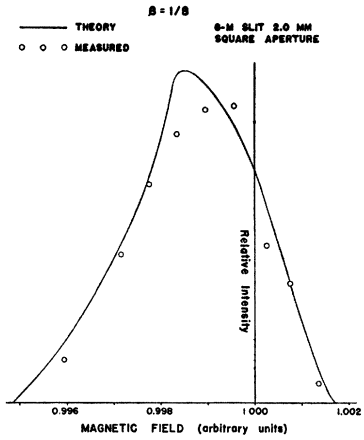

FIG. 3. Apparent line shape from a line source of finite width (0.3 mm) in the prototype spectrometer. Measured points are for the thorium F line. See text for details.

Figure 3 shows the apparent line shape to be expected in the *prototype* spectrometer from a monoenergetic vertical line source of finite width 0.3 millimeter. Into Fig. 3 has gone all the information contained in the corresponding curve of Fig. 2, plus the contribution caused by the term $-5\delta z^2/6a$ in Eq. (4). Superimposed upon the predicted line shape are experimental points from a measurement of the thorium F line. The thorium source used for this experiment was deposited by recoil upon an aluminum wire of 0.3

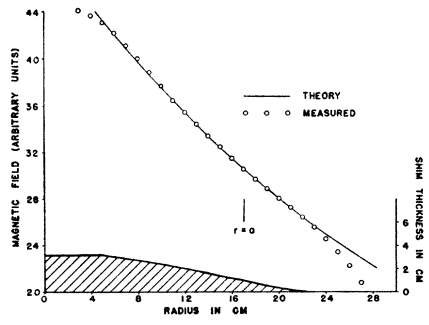

FIG. 4. Comparison of calculated and measured magnetic field shapes, and the contour of one pole shim.

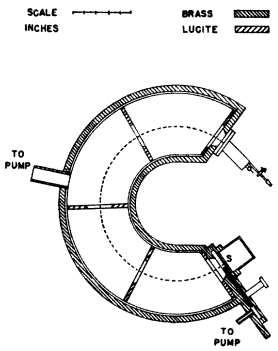

FIG. 5. Simplified drawing of the vacuum chamber.

millimeter diameter. The experimental points have been normalized to an approximate fit with the theoretical line shape. The line shape is not very well confirmed, but the experimental width of the line matches the prediction quite closely. That the predicted line shape is not borne out is not too surprising. As shown in Fig. 3, the experimental points are so closely spaced that variations of only 0.1 percent or less in the magnetic field are necessary to shift from one point to the next. Such small variations demand better accuracy in magnetic field measurements than was feasible.

Frankel[5] has stated that there exists an approximately linear relationship between the resolving power and the transmission factor of a double-focusing spectrometer, where the transmission factor may be defined as the solid angle subtended at the source expressed as a fraction of 4π. That this is so in first approximation for a point source can be seen in Eq. (5) for r^*. The over-all width of the focused image is given by the maximum value of $2a(\varphi_r^2+\varphi_z^2)/3$. Similarly the solid angle subtended at the source is approximately proportional to $(\varphi_r^2+\varphi_z^2)$. Thus both the resolution and the transmission factor are approximately proportional to $(\varphi_r^2+\varphi_z^2)$ and the linear relationship between them is established.

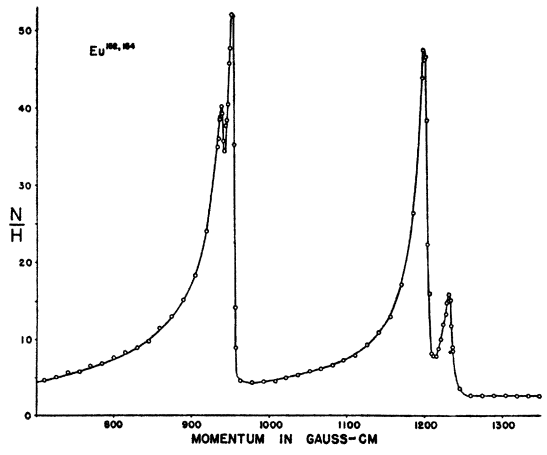

FIG. 6. Internal conversion spectrum of 5–8-year europium, Part 1.

[5] S. Frankel, Phys. Rev. **73**, 804 (1948).

DESIGN OF THE SPECTROMETER

The first step in constructing a double-focusing spectrometer is to provide a magnetic field shaped according to Eq. (1). In the present case there was already available an electromagnet of conventional design, with 22-inch circular plane-parallel pole faces, intended originally for a 180° spectrometer. To adapt this magnet for a double-focusing instrument, the pole spacing was increased to six inches, and a one-piece steel shim of variable thickness was added to each face. Figure 4 shows the thickness of one shim as a function of radius and also a comparison between the shape of the field as required by Eq. (1) and as actually measured. The measured shape of the field is correct for values of H_0 between 2 and 1280 gauss, provided the magnet has first been properly cycled to remove remanence effects. The latter precaution is always observed in normal operation of the spectrometer.

A simplified plan view of the vacuum chamber of the spectrometer is shown in Fig. 5. Its design was governed largely by the requirement that the internal height of the chamber should be as great as possible in order to make maximum use

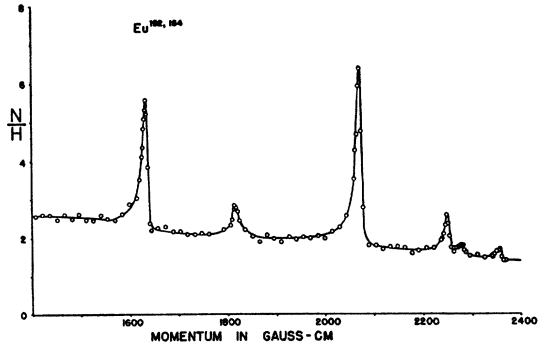

FIG. 7. Internal conversion spectrum of 5–8-year europium, Part 2. Note change of scales.

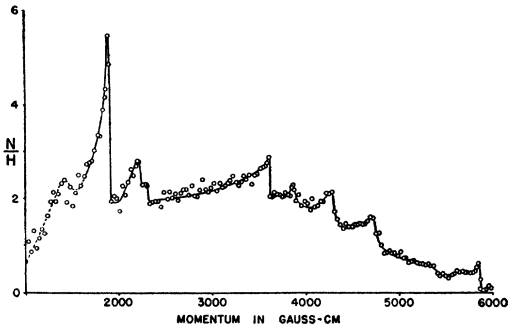

FIG. 8. Photoelectron spectrum of 5–8-year europium, from a Pb radiator.

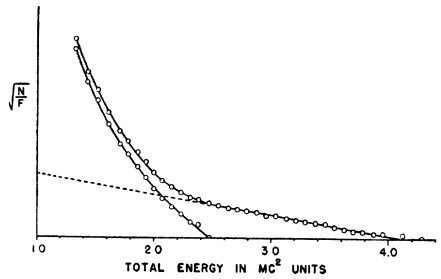

FIG. 9. Fermi plot of the continuous beta-ray spectrum of 5–8-year europium. At least two spectra appear to be present.

of the vertical focusing properties of the shaped magnetic field. Moreover, it was felt that the internal dimensions should be large compared to the cross section of the electron beam so as to minimize wall-scattering troubles within the chamber. The chamber itself is constructed of brass and is lined with thin aluminum sheet. Radial walls, or baffles, of $\frac{1}{4}$-inch Lucite divide the chamber into four compartments of roughly equal volume. Rectangular apertures in the baffles limit the electron beam which can traverse the chamber, and subtend at the source a solid angle of approximately 0.32 percent of 4π steradians. Between the source S and the chamber is interposed a sliding brass shutter, by means of which the source can be isolated from the vacuum whenever it is necessary to remove or change sources. Behind the source, a removable brass cup, lined with cellulose acetate, completes the assembly. The source is so mounted as to keep adjacent metal and plastic surfaces as far removed as possible, thus minimizing trouble caused by secondary electrons engendered by gamma-rays from the source.

Registration of beta-particles is accomplished with an end-fire Geiger tube of conventional cylindrical geometry. The axis of the tube is inclined 8° inward from the normal to the spectrometer wall, so as to give each electron a path length through the effective counting volume of sufficient magnitude to keep the counting efficiency high. Sheet nylon of thickness 0.84 mg/cm^2 was originally used for the counter window. Such a window is opaque to electrons of energy below 30 kev, and passes 72 percent of 64 kev electrons. At the present time, an alternative window is available which permits the extension of measurements down to about 15 kev. This window consists of a collodion film laid over a phosphor bronze supporting grid. A hexagonal array of holes (0.036 inch diameter) in the grid gives 58 percent open area. The useful range for the thin window is from about 15 to 650 kev.

The methods used for controlling and measuring the magnetic field have been described in an earlier paper.[6] As explained there, the electromagnet is supplied from storage batteries, which in turn are trickle-charged by a d.c. generator. The device used for measuring the magnetic field is essentially the armature of a d.c. generator driven by a synchronous motor. The motor in turn is supplied from a d.c.-a.c. thyratron inverter controlled by a locked-frequency audio oscillator. This gives frequency regulation better than that afforded by the regular 110-volt lines. Repeated determinations of the field of a permanent magnet make reasonable the assumption that the magnetic field can be measured with about 0.1 percent relative accuracy. The absolute accuracy is somewhat less certain. The measuring device and the spectrometer were calibrated as a unit by making an observation of the F line in the internal conversion spectrum of thorium B ($H\rho$ assumed 1383.8 gauss-cm). Thus the absolute accuracy contains an additional factor of uncertainty as a result of an uncertainty in the momentum of the thorium F line.

In the course of several months of operation, the performance of the prototype spectrometer has been most gratifying. The high resolution which it affords makes possible the separation of closely-spaced internal conversion peaks, as illustrated by the europium spectrum in Figs. 6

[6] J. M. Cork, R. G. Shreffler, and F. B. Shull, Rev. Sci. Inst. **18**, 315 (1947).

TABLE I.

Ia. Continuous beta-spectra upper energy endpoints

Energy in kev	Relative intensity of spectrum	Identification
751±15	4900	Eu^{152}
1575±150	1200	Could be from either isotope.

Ib. Internal conversion lines

Electron energy in kev	Relative intensity	Possible identifications	Transition energy in kev
73.1	300	*K* conv. in Gd	123.4
74.4	2000	*K* conv. in Gd	124.7
		K photo in Eu	123.0
		K conv. in Sm	121.2
114.0	1740	*L* conv. in Gd	122.4
		L photo in Eu	122.0
		L conv. in Sm	121.7
119.6	330	*M* conv. in Gd	121.5
		M photo in Eu	121.4
		M conv. in Sm	121.3
197.2	70	*K* conv. in Gd	247.5
		K conv. in Sm	244.0
236.1	30	*L* conv. in Gd	244.5
		L conv. in Sm	243.8
		K conv. in Gd	286.4
293.6	90	*K* conv. in Gd	343.9
335.5	17	*L* conv. in Gd	343.9
342.6	8	*M* conv. in Gd	344.5
362.0	4	*K* conv. in Gd	412.3

Ic. Photoelectron lines

Electron energy in kev	Possible identification	Transition energy in kev
155	*K*	243
255	*K*	342
329	*L*, *K*	344, 416
352	*K*	442
684	*K*	772
758	*L*	774
871	*K*	959
995	*K*	1082
1314	*K*	1402

and 7. Moreover, it is possible to establish the existence of low-intensity peaks which would tend to fade into the continuous background in an instrument with lower resolving power. The double-focusing spectrometer also offers advantages in the determination of beta-spectrum shapes as a test of the theory of beta-decay. Recent reports indicate the possibility that the Fermi theory for allowed spectra is not confirmed in the region of very low electron energy. The relatively high transmission factor of a double-focusing spectrometer alleviates somewhat the problem of low counting rates at very low energies. By opening up the baffle apertures, the transmission factor could be increased to facilitate this type of work. This would entail a corresponding decrease in resolving power, but even so, the resolution is still good when compared with a conventional 180° instrument.

The first beta-emitting sources which were examined with the double-focusing spectrometer were selected with a view toward testing the performance of the instrument. One was a long-lived activity in europium which was known to be rich in internal conversion lines. The other was a 75-day activity in tungsten which was known to be a pure beta-emitter. With these it was hoped that the capabilities of the spectrometer in measuring both continuous and line spectra would become evident.

EUROPIUM^{152,154}

When the stable isotopes of europium are irradiated in a neutron pile, active isotopes of atomic weights 152 and 154 are formed by (n, γ) processes. A mass spectrographic analysis by Inghram and Hayden[7] showed that activities can be assigned to these isotopes as follows:

Atomic weight	Half-life
152	9.2 hours
152	5–8 years
154	5–8 years.

The same authors made absorption measurements of the two 5–8 year activities without attempting to distinguish between them, and reported "at least two betas and one gamma." The gamma-energy was given as 1.4 Mev.

The 9.2-hour isomer of Eu^{152} has been studied by Tyler,[8] who used a 180° magnetic spectrometer. He observed a beta-spectrum having an upper energy limit of 1.885 Mev, and internal conversion peaks corresponding to transitions of 123 and 724 kev, all decaying with the 9.2-hour half-life. In addition he noted several indications of other conversion lines, but was unable to resolve them into definite peaks because of the low intensity of his source.

Cork, Shreffler, and Fowler[9] studied the long-

[7] M. G. Inghram and R. J. Hayden, Phys. Rev. **70**, 89; **71**, 130 (1946–47).
[8] A. W. Tyler, Phys. Rev. **56**, 125 (1939).
[9] J. M. Cork, R. G. Shreffler, and C. M. Fowler, Phys. Rev. **72**, 1209 (1947); **73**, 78L (1948).

lived activities of europium in a photographic 180° spectrometer, and reported internal conversion lines corresponding to transitions of 122, 247, 286, 343, and 408 kev. In addition, a 1.23-Mev gamma-ray was indicated by absorption measurements, as well as a continuous beta-spectrum of energy 0.93 Mev.

Wiedenbeck and Chu,[10] using a coincidence-counting technique, reported the continuous beta-spectrum of long-lived europium to be complex, with upper energy limits of 0.62 and 1.0 Mev.

In preparing active europium for the present research, pure Eu_2O_3 was subjected to neutron irradiation in the Oak Ridge pile. Following irradiation, a time lapse of about six months occurred, after which the measurements reported below were undertaken. Thus the 9.2-hour isomer of Eu^{152} was eliminated. Two types of spectra were sought, first an internal conversion line spectrum superimposed on a continuous beta-ray background, and second a photoelectron line spectrum from a lead radiator. The conversion spectrum was determined from a powder source on a substrate of Scotch tape 0.8 millimeter in width. The photoelectron spectrum was determined from a source contained in a lead test tube of one-millimeter bore and one-millimeter wall thickness.

Ten conversion lines and two continuous beta-spectra are observed in the conversion spectrum. Since the conversion lines vary widely in intensity, the over-all spectrum does not lend itself easily to plotting in a single graph. Consequently the spectrum has been broken up into two sections and is plotted to different scales in Figs. 6 and 7. The photoelectron spectrum shows nine peaks and is plotted in Fig. 8. Few of the nine peaks stand out very prominently above the Compton background, and some of them are of dubious reality. The continuous tail of the conversion spectrum can be analyzed by means of a Fermi plot as shown in Fig. 9. Two spectra appear to be superimposed, with energies 0.751 ± 0.015 Mev and 1.575 ± 0.150 Mev. The large uncertainty in the latter is due to extremely low counting rates and very poor statistics. All the data are assembled in tabular form in Table I. Possible identifications, sometimes several of them, are suggested for each conversion or photoelectron peak. In each case, the corresponding nuclear transition energy is given also.

A complete, consistent, and unique interpretation of the internal conversion and the photoelectron line spectra of europium cannot be developed for several reasons. First, the presence of two isotopes, both having approximately the same half-life, makes it almost impossible to show conclusively which radiations are associated with the one and which with the other isotope. Second, the small number of *K-L-M* sets in the conversion spectrum makes it difficult in many cases to decide in which atom the internal conversion process is taking place. Third, purely spectrometric energy measurements cannot give any information about genetic relationships between various nuclear transitions.

Only in one instance is sufficient information known on which to base a strong argument regarding the choice between Eu^{152} and Eu^{154} as the parent of an observed gamma-transition. Tyler[8] found a 1.885-Mev β^--transition and a pair of very strong internal conversion lines at $H\rho=940$ and $H\rho=1186$ in the spectrum of the 9.2-hour isomer of Eu^{152}. In the present investigation of long-lived europium, two β^--spectra were observed, of energy 0.751 and 1.575 Mev; in addition there is a group of very strong conversion lines at $H\rho=938$, 952, 1199, and 1231 gauss-centimeters, of which those underlined are by far the strongest. It seems a reasonable guess that the pair of lines reported by Tyler and the similar lines reported here all result from the same nuclear transition or transitions. The fact that Tyler observed only two lines, as well as the comparatively lower momentum values reported by him, are explainable as being due in part to the rather low resolving power ($\sim$1.5 percent) of his 180° spectrometer.

The following argument can be built upon this similarity between the spectra of 9.2-hour and 5–8-year europium. It may be hypothesized that both isomers of Eu^{152} decay by β^--emission. It is therefore assumed that each of the final states in the two cases (immediately following β^--decay) is a member of a single system of excited states of Gd^{152}. The consequences of this argument would be as follows:

[10] M. L. Wiedenbeck and K. Y. Chu, Phys. Rev. **72**, 1164 (1947).

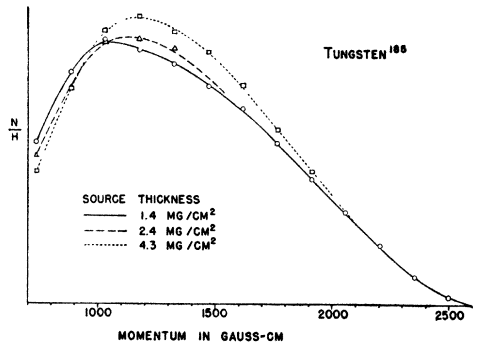

FIG. 10. The continuous beta-ray spectrum of tungsten[185]. Curves are normalized to one another at high energies.

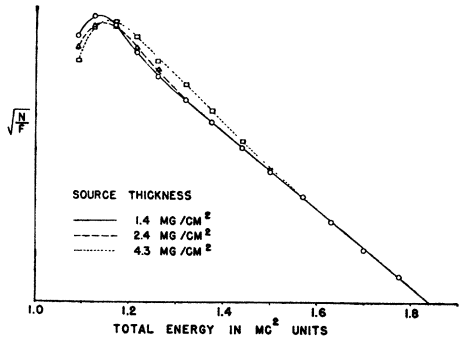

FIG. 11. Fermi plot of the W^{185} beta-spectrum. Curves are normalized to one another at high energies.

(a) The low energy conversion lines observed in 5–8-year europium, which are probably caused by two transitions of approximately equal energy (see further discussion of this point in later paragraphs), must definitely be associated with Eu^{152}, not Eu^{154}.

(b) The 0.751-Mev β^--spectrum of 5–8-year europium must also be associated with Eu^{152}, inasmuch as the much smaller population of the 1.575-Mev spectrum is insufficient by itself to account for the large population of the conversion lines, i.e., the conversion coefficient would then turn out to be greater than unity.

(c) The relative populations of the low-energy conversion lines and of the 0.751-Mev β^--spectrum suggest that the total internal conversion coefficient for at least one of the two alleged transitions is very large, perhaps as large as 80 percent.

(d) By inference, one can draw the much weaker conclusion that some, perhaps all, of the other conversion peaks and gamma rays observed in 5–8-year europium may also be due to transitions in gadolinium following a β^--transition. This argument is included because it is apparent from Table I that assignments of some of the other observed radiations to transitions in gadolinium are either refuted by consideration of the *K-L-M* energy differences or cannot be made at all because of the failure to observe *K-L-M* sets. In particular, it appears in two instances that *K-L-M* or *K-L* differences are found which are most nearly characteristic of samarium. This would require decay of europium either by positron (β^+) emission or *K*-capture. Neither positron emission nor annihilation radiation are found in 5–8 year europium. *K*-capture is still a possibility, but proof of its occurrence could only be obtained through a search for the characteristic samarium x-rays which would accompany it.

Another point of interest in the europium conversion spectrum concerns the interpretation to be placed upon the four peaks of lowest energy. It has been suggested by Cork, Shreffler, and Fowler[9] that all four peaks are the result of a single nuclear transition in gadolinium following a β^--transition from europium. It is assumed that this transition may result either in (a) the direct emission of internal conversion electrons from gadolinium, or in (b) the emission from gadolinium of a gamma-ray which ejects photoelectrons from neighboring europium atoms. Either process could produce a complete group of *K-L-M* peaks. The excitation potentials of gadolinium and europium are such that only the two *K* peaks would differ sufficiently in energy to be resolvable. Thus four distinct peaks would be observed. As indicated in Table I, however, the data reported here do not yield consistent values for the transition energy when interpreted in the above fashion.

Another plausible explanation of these four low-energy conversion peaks is to assume that they are conversion lines resulting from two distinct nuclear transitions of very nearly the same energy. If this be the case, the relative intensities of the two *K* peaks should remain the same when the radioactive sample is made thinner and weaker. In contrast, the mechanism suggested by Cork, Shreffler, and Fowler would require the relative intensities of the two *K* peaks to alter

in favor of the conversion peak when the sample is made thinner and weaker. In order to discover which interpretation is more plausible, this section of the conversion spectrum was remeasured, using a sample whose mass per unit area was about 0.3 times that used originally. No marked alteration was observed in the relative intensities of the two K peaks. It is concluded that the mechanism suggested by Cork, Shreffler, and Fowler is less plausible than the alternative one which requires that two separate nuclear transitions take place.

The presence of two indistinguishable isotopes and the absence of information concerning the genetic relationships of the beta- and gamma-rays from europium make it impossible to reason out a plausible energy level scheme which will account for the observed radiations. Some attempts in this direction have been made, but the results are unquestionably dubious. For instance, if one were to assume that eleven gamma-transitions take place all in one type of nucleus, with gamma-energies of 123, 124, 247, 286, 344, 412, 442, 772, 959, 1082, and 1402 kev, a system of seven energy levels (including the ground level) can be found which might account for them within one or two kev accuracy. This system would have levels at 123, 247, 533, 877, 1206, and 1649 kev above the ground level. However, a series of experiments involving coincidence spectrometry will be necessary before any acceptable conclusions can be drawn with respect to an energy-level diagram.

TUNGSTEN^{185}

Tungsten has five stable isotopes of atomic weights 180, 182, 183, 184, and 186. Minakawa[11] and Fajans and Sullivan[12] investigated the activities induced in tungsten by slow neutron bombardment, and discovered two activities of 24-hour and about 75-day half-life, which they attributed to W^{187} and W^{185} respectively. Minakawa reported W^{185} to be a beta-emitter, with an upper energy limit of 0.4–0.5 Mev based on aluminum absorption measurements. Fajans and Sullivan found the upper energy limit of W^{185} to be 0.55–0.65 Mev on the basis of absorption data, and 0.64–0.72 Mev as a result of preliminary cloud-chamber work. A later paper by Sullivan[13] placed the limit at 0.55 Mev on the basis of more complete absorption data, and reported also that no gamma-rays could be detected. Jnanananda[14] measured the beta-spectrum of W^{185} in a lens type spectrometer, and observed the upper limit at 0.675 Mev. There is considerable suspicion that this high value was due to the presence of a small contaminant of iridium in his sample. Saxon[15] also investigated tungsten with a lens spectrometer and reported the energy limit as 0.43 Mev.

The samples from which the W^{185} beta-spectrum was measured were obtained by neutron irradiation of tungsten oxide. Samples were prepared by allowing the finely powdered oxide to fall out of a water suspension onto a substrate of nylon of thickness 0.84 mg/cm^2. The spectrum was measured three times, from samples of thickness 1.4, 2.4, and 4.3 mg/cm^2, respectively. The measured spectra, normalized to coincide with one another at high energies, are plotted as functions of momentum in Fig. 10, and the corresponding Fermi plots appear in Fig. 11. It is immediately obvious that the low energy portions of the spectrum are markedly subject to self-scattering effects within the sample. An extrapolation of the Fermi plot to its intersection with the energy axis yields a value for the transition energy of 1.84 mc^2 or 0.428 Mev, which agrees very well with the determination made by Saxon.

According to the lifetime-energy criterion developed by Konopinski[16] the W^{185} beta-transition falls into a category of twice-forbidden transitions. From the data obtained with the thinnest sample, it appears that the spectrum has the allowed shape down to energies somewhat less than 150 kev. Below this energy it is quite possible that experimental difficulties contribute to the observed deviations.

ACKNOWLEDGMENTS

The author is deeply grateful to the Eastman Kodak Company for fellowship support during the 1947–8 academic year. The spectrometer project was sponsored and supported by the Office of Naval Research.

[11] O. Minakawa, Phys. Rev. **57**, 1189L (1940).
[12] K. Fajans and W. H. Sullivan, Phys. Rev. **58**, 276 (1940).
[13] W. H. Sullivan, Phys. Rev. **68**, 277 (1945).
[14] S. Jnanananda, Phys. Rev. **72**, 1124 (1947).
[15] D. S. Saxon, private communication to S. Jnanananda.
[16] E. J. Konopinski, Rev. Mod. Phys. **15**, 209 (1943).